NJC

Accepted Manuscript

This is an *Accepted Manuscript*, which has been through the Royal Society of Chemistry peer review process and has been accepted for publication.

Accepted Manuscripts are published online shortly after acceptance, before technical editing, formatting and proof reading. Using this free service, authors can make their results available to the community, in citable form, before we publish the edited article. We will replace this *Accepted Manuscript* with the edited and formatted *Advance Article* as soon as it is available.

You can find more information about *Accepted Manuscripts* in the Information for Authors.

Please note that technical editing may introduce minor changes to the text and/or graphics, which may alter content. The journal's standard Terms & Conditions and the Ethical guidelines still apply. In no event shall the Royal Society of Chemistry be held responsible for any errors or omissions in this *Accepted Manuscript* or any consequences arising from the use of any information it contains.

ROYAL SOCIETY OF CHEMISTRY

www.rsc.org/njc

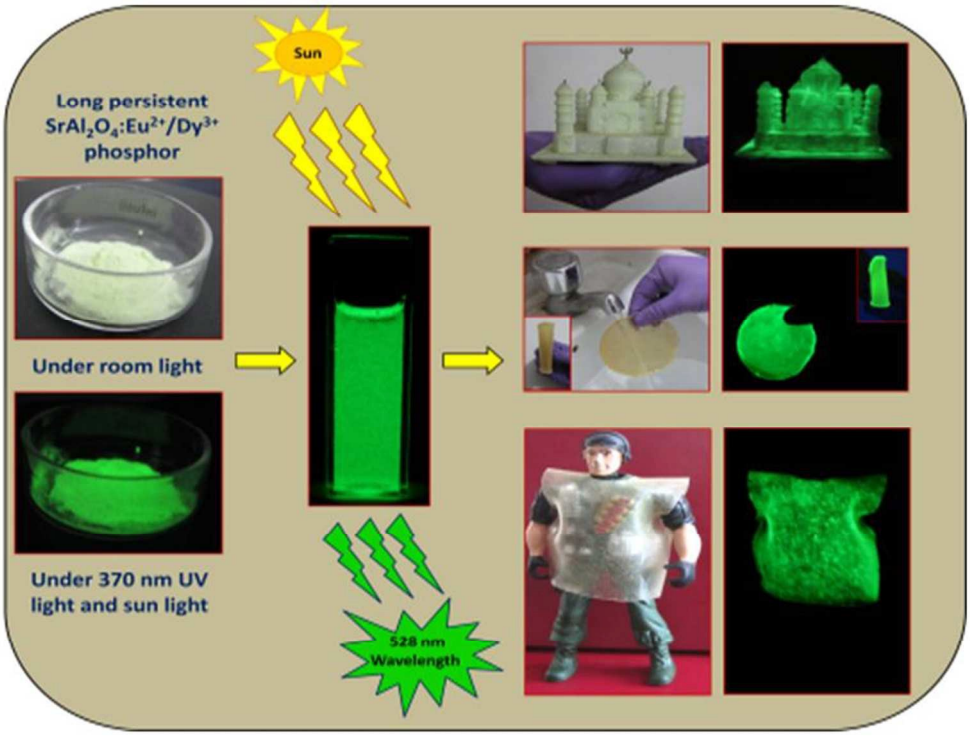

Demonstration of a high brightness, strong green emitting, water resistant and flexibile phosphorescent layer for display and defence applications.
254x190mm (96 x 96 DPI)

Cite this: DOI: 10.1039/c0xx00000x

www.rsc.org/xxxxxx

ARTICLE TYPE

Sunlight-activated Eu^{2+}/Dy^{3+} doped $SrAl_2O_4$ water resistant phosphorescent layer for optical display and defence applications

Arun Kumar[a], Garima Kedawat[b], Pawan Kumar[a], Jaya Dwivedi[a] and Bipin Kumar Gupta[*,a]

Received (in XXX, XXX) XthXXXXXXXXX 20XX, Accepted Xth XXXXXXXXX 20XX

DOI: 10.1039/b000000x

Herein, we introduce a strategy for the fabrication of sunlight-activated green luminescent Eu^{2+}/Dy^{3+} doped strontium aluminate ($Sr_{1-x-y}Al_2O_4$: Eu_x^{2+}/Dy_y^{3+}) assisted long persistent, transparent, flexible and water **resistant** phosphorescent layer via customized solid state reaction-solution cast method. The XRD result of as-synthesized phosphor shows the pure monoclinic crystal structure with space group $P2_1$. This as-synthesized phosphor exhibits green afterglow emission with broad band peaking ~528 nm upon a broad range of excitation wavelengths from 368-418 nm, which is ascribed to the characteristic $4f^65d^1 \rightarrow 4f^7$ electronic dipole allowed transition of Eu^{2+} ions. Moreover, the role of Dy^{3+} as an auxiliary activator significantly prolongs the afterglow duration to a large extent by increasing the number of electron traps and their trap depths in the vicinity of Eu^{2+}. Accordingly, brighter afterglow intensity with longer time more than 5 hours is observed for the optimal concentration of Eu^{2+}/Dy^{3+} in $Sr_{1-x-y}Al_2O_4:Eu_x^{2+}/Dy_y^{3+}$, (x=0.1 and y=0.2) long persistent phosphor. The incorporation of sunlight-activated as-synthesized $Sr_{0.7}Al_2O_4:Eu_{0.1}^{2+}/Dy_{0.2}^{3+}$ phosphor in commercial available PVC gold medium offers a highly dispersive transparent luminescent paint, which can be used for spray coating of monuments as well as for the fabrication of transparent, flexible and water **resistant** phosphorescent layer. Hence, these striking features of luminescent paint as well as flexible transparent phosphorescent layer could be potentially utilized in optical display and defence applications.

1. Introduction

Phosphorescent materials with long afterglow are a kind of energy storage materials in the form of trapped electrons and holes, which can absorb both ultraviolet (UV) and visible lights from the sunlight and progressively release the energy through the slow de-trapping and radiative recombination of the carriers at a certain wavelength in the visible region.[1] Recently, these kind of long persistent phosphor (LPP) materials have been widely considered much attention[1,2] owing to its reusable energy storage property and have been extensively applied in emergency signing, decorative purposes and escape route indicators,[3-5] bio imaging detection,[6] high energy radiation detection[7] and in energy saving devices like solar cell applications.[8-10] The research and development of LPPs has led to the commercialization of each primary color emitters, such as blue ($CaAl_2O_4:Eu^{2+}/Nd^{3+}$ and $SrMgSi_2O_6:Eu^{2+}/Dy^{3+}$)[11,12], green ($SrAl_2O_4:Eu^{2+}/Dy^{3+}$ and $MgAl_2O_4:Mn^{2+}$)[13,14] and red ($Y_2O_2S:Eu^{3+},Mg^{2+}/Ti^{4+}$ and $CaS:Eu^{2+}/Tm^{3+}/Ce^{3+}$)[15,16] phosphors. The strontium aluminate based phosphors have replaced the conventional sulphide (eg; ZnS) based phosphorescence materials due to non-radioactive, high emission intensity, long-lasting phosphorescence and their good chemical and thermal stability.[17]

The Eu^{2+}/Dy^{3+} doped strontium aluminate phosphor with wide band gap has paying intensive scientific research owing to its emission band in blue and green regions[18] and discovered in 1996.[13] This phosphor has several crystallizes phases such as $SrAl_2O_4$, $SrAl_4O_7$, $SrAl_{12}O_{19}$, $Sr_4Al_{14}O_{25}$ and $Sr_2Al_6O_{11}$, where the $SrAl_2O_4$ (SAO) exhibits two polymorphs: monoclinic and hexagonal.[19] This is because, in $SrAl_2O_4$ host, Sr^{2+} ions are located in the cavities of the frame work of $[AlO_4]^{5-}$ tetrahedral, occupying two dissimilar sites with low symmetry and coordinated by nine oxygen atoms.[20] The green phosphorescence is observed for $SrAl_2O_4:Eu^{2+}/Dy^{3+}$ phosphor based on the hole-trapping mechanism, which suggested that the activated Eu^{2+} in its energized 5d state releases a hole to the valence band leaving behind the Eu^{1+} ion. The hole is then trapped by Dy^{3+} leaving behind the Dy^{4+} ion. The thermal energy causes the release of trapped hole to the valence band again, and it moves back to a Eu^{1+} ion, allowing the excited Eu^{1+} ion to return to the Eu^{2+} ground state, whereby the emission of a

photon takes place.[21] The energy transfer process from a sensitizer (Eu^{2+}) to an activator (Dy^{3+}) can improve the afterglow property due to the introduction of the defects, which is benefited to prolong the afterglow duration. This gives rise to a visible-light emission lasting for minutes or hours, as for many applications in night or dark environment vision displays. These particulars have resulted in unprecedented success of $SrAl_2O_4:Eu^{2+}/Dy^{3+}$ phosphor for applications as luminescent pigments. It can be used in safety and emergency signs, as well as in luminous painting in watches and other instruments' dials.[22-25]

Herein, we have synthesized $Sr_{1-x-y}Al_2O_4:Eu_x^{2+}/Dy_y^{3+}$ phosphor via the conventional solid state reaction method at 1300 °C under reducing atmosphere of 10% H_2 and 90% N_2. **The purpose of the adoption of solid state reaction route in present investigations is due to the fact that this method is widely accepted for synthesis of phosphor material for commercial applications as compared to other methods like sol-gel, hydrothermal and auto-combustion etc. Additionally, the synthesis of phosphor using this method demonstrates good brightness with higher quantum yield, higher luminescent intensity as compared to the other methods. In addition to this, the solid reaction is one step process which generally occurred at high temperature for large scale production and phosphors are easily reproducible using this method, while other methods need to number of synthesis run to produce large scale quantity. This may be also affect the homogeneity and uniformity of phosphor, whereas in case of solid state reaction, this kind of problem is almost negligible due single step synthesis process.** The morphology, micro-structural and photoluminescence properties of the synthesized phosphor have been characterized in details. In order to develop a luminous paint, the as-synthesized long persist phosphor was further homogenously mixed with PVC gold medium; **the composition of PVC gold medium is polyvinyl chloride resin + cyclo hexanone + nitrobenzene + ethyl cellulose+ C_9 reducer (aromatic hydrocarbon solvent). However, few reports on security applications are existing, which is based on phosphor with PVA (polyvinyl alcohol), sodium hexametaphosphate (SHMP), cyclohexane and poly methyl methacrylate (PMMA) but no one attempt to use commercial available PVC gold medium at economic cost which act here as a magic medium and have capability to disperse the phosphor in medium. Additionally, the viscosity of the PVC gold medium (3000 μP) is very important as it provides the sticky nature for the applications like coating on object, printing and many others. Furthermore, the PVC gold medium has porous nature, which helps to pigments the phosphor inside the pores. PVC gold medium was used to fabricate layer due to easily available in market at low cost and it contains several required properties, which essential for proposed applications. This thick transparent solution was coated as a luminescent paint on ceramic monument via spray machine for optical display applications. Furthermore, this transparent solution is converted into a phosphorescent, flexible and water resistant layer through solution casting method for jacket design in defence applications. The proposed composite layer structure (PVC gold medium + $SrAl_2O_4:Eu^{2+}/Dy^{3+}$ phosphor) that has flexibility, transparency and water-resistant properties is proposed first time which is not reported so far.**

2. Experimental section

2.1. Synthesis of long decay $Sr_{1-x-y}Al_2O_4:Eu_x^{2+}/Dy_y^{3+}$ (x=0.05 to 0.3, y=0.1 to 0.6) phosphor.

A strontium aluminate phosphor doped with Eu^{2+}/Dy^{3+} ions ($Sr_{1-x-y}Al_2O_4:Eu_x^{2+}/Dy_y^{3+}$; x= 0.05 to x=0.3 and y=0.1 to 0.6) was synthesized using an efficient and customized solid state reaction method. Initially, all the raw materials, strontium carbonate ($SrCO_3$; Sigma Aldrich, 99.9%), aluminium oxide (Al_2O_3; Sigma Aldrich, 99.9%), europium oxide (Eu_2O_3; Sigma Aldrich, 99.9%) and dysprosium oxide (Dy_2O_3; Sigma Aldrich, 99.9%) with molar ratio of 0.7:2.00:0.1:0.2 for Sr:Al:Eu:Dy were mixed thoroughly and grinded in a mortar- pestle using a little amount of ethanol to make a fine powder with intermediate mixings and groundings. The well-mixed composition was put in an alumina crucible, which were introduced into a muffle furnace and heated at a rate of 5 °C/min and maintained at 1300 °C for 3 hrs under reducing atmosphere comprising 10% H_2 and 90% N_2 to get the desired phosphor material. Then, the sample was cooled to ambient temperature in the furnace. The as-obtained the yellowish white product in the powder form was grinded finely having more than 90% yield and it is used for characterization and photoluminescence (PL) measurements. The protocol for synthesis of afterglow phosphor ($Sr_{1-x-y}Al_2O_4:Eu_x^{2+}/Dy_y^{3+}$; x= 0.05 to x=0.3, y=0.1 to 0.6) by solid state reaction method is given in Scheme S1 (see supplementary information). We have carried out the experiment with different concentration of Eu^{2+}/Dy^{3+} ($Sr_{1-x-y}Al_2O_4:Eu_x^{2+}/Dy_y^{3+}$; x= 0.05 to x=0.3, y=0.1 to 0.6) keeping correspondingly change in Dy. The nominal $Sr_{1-x-y}Al_2O_4:Eu_x^{2+}/Dy_y^{3+}$; x= 0.05 to x=0.3, y=0.1 to 0.6 compositions are detailed in Table S1. The charge compensators used in the present study are HBr and HBO_3 as flux. The PL spectra for different concentration of Eu, Dy substitution in place of Sr are given in Fig. S1 (see supplementary information). The optimum sample ($Sr_{0.7}Al_2O_4:Eu_{0.1}^{2+}/Dy_{0.2}^{3+}$ phosphor) has shown better PL intensity in compare to other compositions, which is further, explained in detailed in PL section.

2.2. $Sr_{1-x-y}Al_2O_4:Eu_x^{2+}/Dy_y^{3+}$ phosphor for display applications.

The successfully as-synthesized $Sr_{1-x-y}Al_2O_4:Eu_x^{2+}/Dy_y^{3+}$ yellowish white colored phosphor powder was further used to obtain the phosphorescent paint. 1 gm of $Sr_{0.7}Al_2O_4:Eu_{0.1}^{2+}/Dy_{0.2}^{3+}$ phosphor is mixed within 500 mL

paint based PVC gold medium and sonicated it for 1 hr at 25 kHz frequency. Once, the powder was homogeneously mixed with PVC gold medium, the transparent colored thick mixture solution was obtained. The colloidal solution with transparency ~76% was obtained and the transmittance spectrum is shown in Fig. S2 (see supplementary information) and inset depicts the optical image of prepared solution, which contributes the formation of scattering-free luminescent film. The afterglow luminous paint was coated using spray machine onto ceramic based Tajmahal monument for optical display applications.

2.3. $Sr_{1-x-y}Al_2O_4:Eu_x^{2+}/Dy_y^{3+}$ phosphor as flexible, transparent, water resistant phosphorescent layer for defence applications.

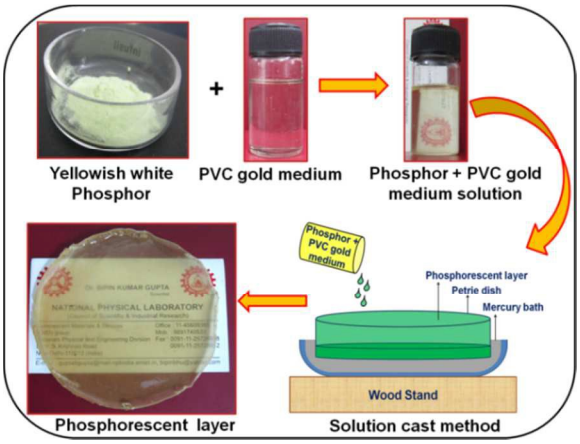

Fig. 1. The schematic representation of preparation method of phosphorescent layer of prepared transparent solution using solution cast method.

The as-obtained 50 mL transparent solution was further sonicated for 30 min at 25 kHz frequency. The phosphorescent layer was obtained by casting the homogeneous solution in petri dish floating on mercury using solution cast method. The layer of uniform thickness (1.0±0.04) mm was prepared and dried under vacuum to eliminate the residual solvent. The schematic representation of preparation method of phosphorescent layer of prepared transparent solution using solution cast method is shown in Fig. 1.

2.4 Characterization

The phase identification and gross structural analysis of synthesized $Sr_{1-x-y}Al_2O_4:Eu_x^{2+}/Dy_y^{3+}$ phosphor was carried out using the X-ray diffraction (XRD) technique, on a PANalytical X'pert PRO X-ray Diffractometer instrument with Cu-$K\alpha_1$ radiation of λ=1.5406 Å at room temp. Raman spectra were obtained using Renishaw 25 InVia Raman spectrometer, UK with an excitation source of 514.5 nm. Fourier transforms infrared (FTIR) spectroscopic measurements were performed on a Thermo Scientific FTIR spectrometer (model: NICOLET 6700). The XPS analysis was carried out in an ultra-high vacuum (UHV) chamber equipped with a hemispherical electron energy analyzer (Perkin Elmer, PHI1257) using nonmonochromatized Al Kα source (excitation energy of 1486.7 eV) with a base pressure of $4x10^{-10}$ torr at room temperature. Contact angle measurement were carried out drop shape analysis system DSA 10 Mk2. Scanning Electron Microscopy (SEM) observations were performed using a Carl ZEISS EVOR-18 instrument with operating source at 10kV. For microstructural analysis, transmission electron micrographs (TEM) were performed by JEOL JEM 200 CX model operated at 200kV. UV-Visible spectra were collected using a high resolution UV-Vis spectrophotometer (MODEL No.LS 55). The Photoluminescence (PL) characterizations were measured using photoluminescence spectrometer (Edinburgh FLSP-920) equipped with a xenon lamp as an excitation source. CIE color measurement was done by the spectrophotometric method using the spectral energy distribution of the given sample and then calculating the CIE color coordinates x and y. Before afterglow measurements; the phosphor sample was exposed to 450W xenon lamp for 10 minutes. The decay curves were obtained using kinetics decay measurements with the photoluminescence spectrometer (Edinburgh FLSP-920). The contact angle measurement was carried out using drop shape analysis system DSA 10 Mk2. All the measurements were carried out at room temperature. The as-obtained $Sr_{1-x-y}Al_2O_4:Eu_x^{2+}/Dy_y^{3+}$ phosphor powder and transparent and flexible phosphorescent layer was excited by the long wavelength of 370 nm UV Lamp and sunlight respectively, for all the proposed applications. The phosphorescent images were recorded using green sensitive Nikon high resolution digital camera.

3. Results and discussion

3.1. Structural Analysis

The as-synthesized long decay $Sr_{1-x-y}Al_2O_4:Eu_x^{2+}/Dy_y^{3+}$ (x=0.05 to 0.3, y=0.1 to 0.6) phosphor powder was obtained in yellowish white color. The optimum concentration of the sample was obtained for x=0.1 and y=0.2 with stoichiometric formula $Sr_{0.7}Al_2O_4:Eu_{0.1}^{2+}/Dy_{0.2}^{3+}$, which can be clearly seen in Fig. S1 (PL spectra; see supplementary information). The phase purity, crystallite size and crystallinity of synthesized phosphor powder play great influence on the PL properties. XRD technique was used to characterize the gross structural analysis as well as phase purity of the synthesized phosphor powder. Before the XRD measurement, the diffractometer was calibrated with silicon powder (d_{111}=3.1353 Å).[26] The XRD pattern of $Sr_{0.7}Al_2O_4:Eu_{0.1}^{2+}/Dy_{0.2}^{3+}$ phosphor sample is depicted in Fig. 2a. As can be seen, the diffraction peaks match well with the JCPDS card No. 74-0794, indicating that the pure monoclinic crystal structure with space group $P2_1$ is obtained. The co-doping Eu^{2+} and Dy^{3+} do not cause any significant change in the host structure. The lattice parameters for $Sr_{0.7}Al_2O_4:Eu_{0.1}^{2+}/Dy_{0.2}^{3+}$ were calculated from the observed d values as-obtained by a least square fitting method by computer program based 'unit cell refinement software'.[27] The estimated cell parameters are a = (8.4021±0.0011) Å, b = (8.7984±0.0019)

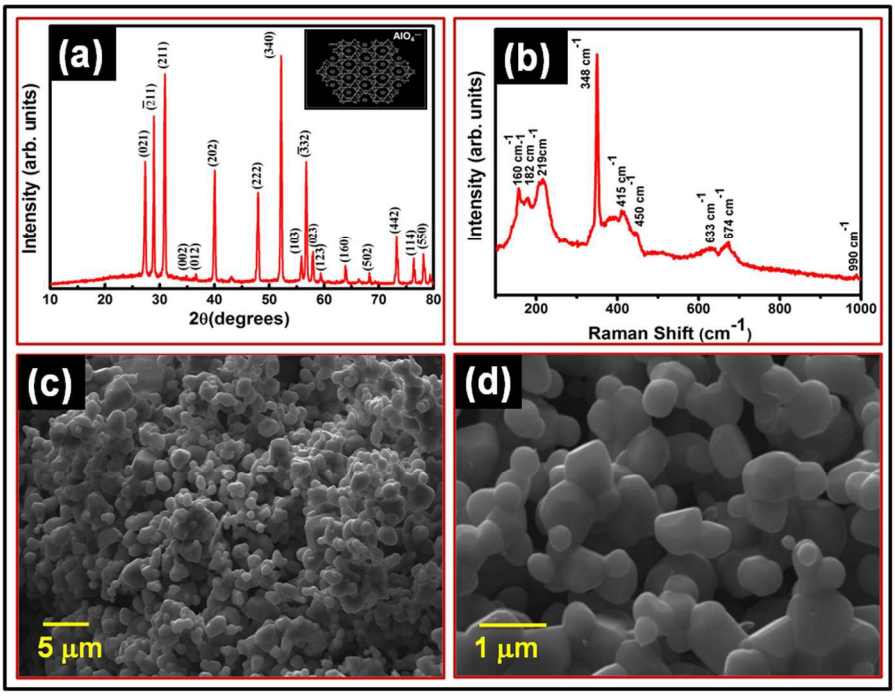

Fig. 2: (a) the XRD pattern of $Sr_{0.7}Al_2O_4:Eu_{0.1}^{2+}/Dy_{0.2}^{3+}$ phosphor sample, which indicate the pure monoclinic crystal structure with space group $P2_1$ and inset displays the three-dimensional crystal structure sketch of $SrAl_2O_4$ with a stuffed β-tridymite type structure, (b) the Raman spectrum of $Sr_{0.7}Al_2O_4:Eu_{0.1}^{2+}/Dy_{0.2}^{3+}$ phosphor, (c) a typical SEM image of $Sr_{0.7}Al_2O_4:Eu_{0.1}^{2+}/Dy_{0.2}^{3+}$ phosphor and (d) magnified view of Fig. 2c, which clearly demonstrates the spherical solid ball like fine structures connected with each other.

Å and c = (5.1469±0.0023) Å. The crystallite size of the sample was calculated from X-ray peak broadening of the diffraction using Scherer's formula and it is found to be **~(0.5±0.01) μm.** The $SrAl_2O_4$ with a stuffed β-tridymite type structure belongs to the monoclinic $P2_1$ space group[28] and its corresponding three-dimensional crystal structure sketch is displayed in inset of Fig. 2a. The Sr^{2+} ions are situated in the cavities of the framework of corner-sharing AlO_4^{5-} tetrahedral. Each oxygen atom is shared with two aluminium ions so that each tetrahedron has one net negative charge. The charge balance is accomplished by the Sr^{2+} ions, which occupy interstitial sites within the tetrahedral framework.[29] The Eu^{2+}/ Dy^{3+} ions have a tendency to occupy the Sr site due to their similar ionic radii and charges.

The Raman spectroscopy has been performed to confirm the crystallinity of $Sr_{0.7}Al_2O_4:Eu_{0.1}^{2+}/Dy_{0.2}^{3+}$ phosphor. Fig. 2b shows the Raman spectrum of $Sr_{0.7}Al_2O_4:Eu_{0.1}^{2+}/Dy_{0.2}^{3+}$ phosphor in a spectral range of 100-1000 cm^{-1} using the 514.5 nm excitation wavelength from a continuous wave Ar^+ laser at room temperature. It confirms the less than 10 active modes, which are partially due to the possible overlap of some symmetry vibrations or the weak features of some Raman bands. The main vibration band attributes to the O–Al–O bonds in corner-sharing tetrahedra, indicating the synthesized material by conventional solid state reaction and exhibits the $P2_1$ monoclinic structure, which is consistent with the XRD results. Furthermore, we also employed the FTIR studies to analyze qualitatively presence of functional group and chemical bonds in the phosphor powder. The FTIR spectrum of the $Sr_{0.7}Al_2O_4:Eu_{0.1}^{2+}/Dy_{0.2}^{3+}$ phosphor is shown in Fig. S3 (see supplementary information). XPS analysis was used to determine the purity and surface properties of the materials. The XPS full scan spectrum of $Sr_{0.7}Al_2O_4:Eu_{0.1}^{2+}/Dy_{0.2}^{3+}$ phosphor powder is shown in Fig. S4 (see supplementary information). It exhibits a binding energy survey scan, which is recorded with pass energy 100 eV. The XPS spectrum specifies the presence of Sr, Al, Eu, Dy and O elements in $Sr_{0.7}Al_2O_4:Eu_{0.1}^{2+}/Dy_{0.2}^{3+}$ phosphor.

3.2. Surface morphology and microstructural analysis

In order to determine the morphology and crystallite size of the synthesized sample, typical SEM measurements were carried out. Fig. 2c displays a typical SEM image of the as-prepared $Sr_{0.7}Al_2O_4:Eu_{0.1}^{2+}/Dy_{0.2}^{3+}$ phosphor annealed at high temperature (1300 °C) under reducing atmosphere and its magnified view is represented in Fig. 2d. It clearly demonstrates the spherical solid ball like fine structures connected with each other. It can be seen that the as-formed precursor consists of uniform and smooth crystalline spherical shape particle with relative average size **~(0.5±0.006) μm.** The prepared particles kept their original morphology and free-standing nature. The particle morphology influences the photoluminescence intensity of the phosphorescent material. The as-synthesized spherical particles show higher photoluminescence intensity compared with that of the irregular-shaped particles.

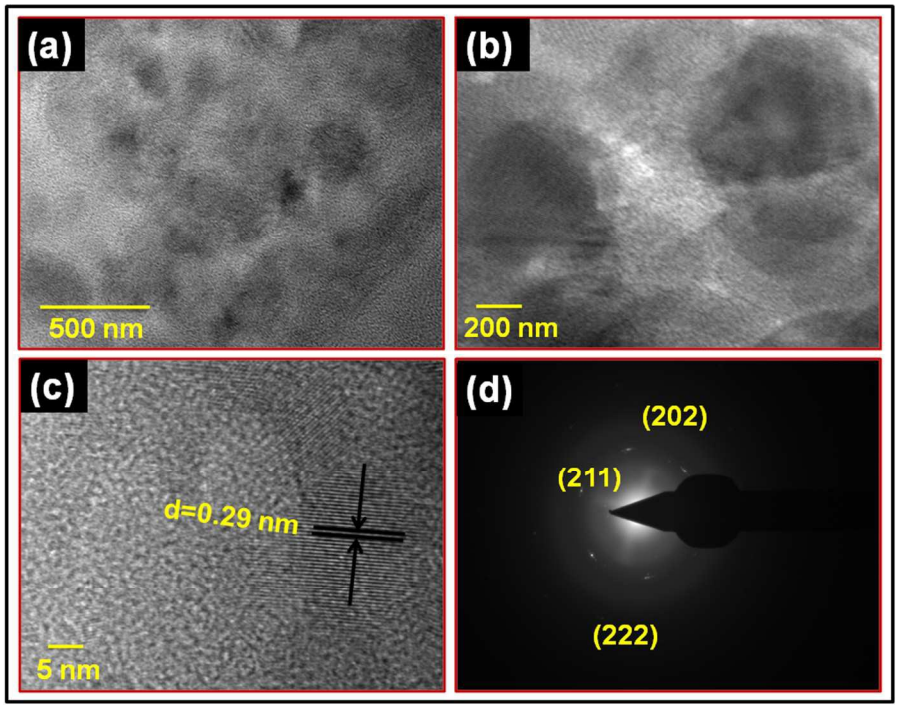

Fig. 3: (a) TEM image of $Sr_{0.7}Al_2O_4:Eu_{0.1}^{2+}/Dy_{0.2}^{3+}$ phosphor, (b) its magnified view; it exhibits the spherical structure of particles, (c) a typical crystalline HRTEM image of $Sr_{0.7}Al_2O_4:Eu_{0.1}^{2+}/Dy_{0.2}^{3+}$ phosphor, which indicates that the interplaner spacing between the lattice fringes is ~0.296 nm, which corresponds to the d spacing for the (211) lattice planes of the monoclinic $SrAl_2O_4$ system and (d) the selected area electron diffraction pattern of $Sr_{0.7}Al_2O_4:Eu_{0.1}^{2+}/Dy_{0.2}^{3+}$ phosphor, the diffraction spots could be indexed as monoclinic phase with lattice planes (202), (211) and (222).

To examine the microstructural information as well as quality of $Sr_{1-x-y}Al_2O_4:Eu_x^{2+}/Dy_y^{3+}$ phosphor, we performed the TEM/HRTEM morphology analysis. For better TEM images, the $Sr_{0.7}Al_2O_4:Eu_{0.1}^{2+}/Dy_{0.2}^{3+}$ phosphor was disseminated in ethanol solution for ~30 minutes and a drop of the as-obtained mixed solution was placed on the carbon coated grid surface. Figs. 3a and 3b represents the TEM image of $Sr_{0.7}Al_2O_4:Eu_{0.1}^{2+}/Dy_{0.2}^{3+}$ phosphor and its magnified view. It exhibits the spherical structure of particles, which has good agreement with previous SEM morphology results. The average particle size estimated from TEM image is **~(0.5±0.001) µm.** Fig. 3c shows the typical crystalline HRTEM image of $Sr_{0.7}Al_2O_4:Eu_{0.1}^{2+}/Dy_{0.2}^{3+}$ phosphor. It indicates that the interplaner spacing between the lattice fringes is 0.296 nm, which corresponds to the d spacing for the (211) lattice planes of the monoclinic $SrAl_2O_4$ system. The selected area electron diffraction (SAED) pattern of $Sr_{0.7}Al_2O_4:Eu_{0.1}^{2+}/Dy_{0.2}^{3+}$ phosphor is depicted in Fig. 3d. It is consistent with the high crystallinity and ordered in crystallography. The diffraction spots could be indexed as monoclinic phase with lattice planes (202), (211) and (222), which are in good agreement with the results of XRD.

3.3. Spectroscopic analysis

The photoluminescence spectroscopic is an essential characterization technique for the determination of electronic energy band structure along with analysis of surface defects. Fig. 4a exhibits the excitation spectrum of $Sr_{0.7}Al_2O_4:Eu_{0.1}^{2+}/Dy_{0.2}^{3+}$ phosphor at 528 nm emission wavelength. It consist a single broad excitation band from 325 to 450 nm, presenting the maximum intensity peak at 368 nm. The excitation spectrum strongly overlaps with the UV–visible portion of solar radiation received at the Earth's surface. This overlap signifies that the as-synthesized phosphor can be efficiently energized by variety of illumination sources, especially, by most common natural sun light. Meanwhile, excitation of 368 nm yields a single strong green emission band of the $Sr_{0.7}Al_2O_4:Eu_{0.1}^{2+}/Dy_{0.2}^{3+}$ phosphor peaking at 528 nm wavelength, as given in Fig. 4b. The greenish emission is ascribed to the $4f^65d^1 \rightarrow 4f^7$ electronic dipole allowed transition of Eu^{2+} ions located inside the $SrAl_2O_4$ host. No emission peaks of Eu^{3+} are obtained in the emission spectra, resulting that Eu^{3+} ion in the samples has been completely get reduced to Eu^{2+} ions. The 4f electrons in Eu^{2+} are well shielded by the outer shell, but the 5d electrons are viable to splitting by the action of crystal field strength. Moreover, the role of Dy^{3+} as an auxiliary activator significantly prolongs the afterglow duration by increasing the number of electron traps and their trap depths in the vicinity of Eu^{2+}. Emission from a certain energy level can occur when the energy gap to the next lower level is more than four or five times the maximum phonon energy of the host lattice. If the energy gap is smaller, the n multi-phonon relaxation occurs and emission is no longer seen.[30] In general, it can be said that there are two factors that influences the

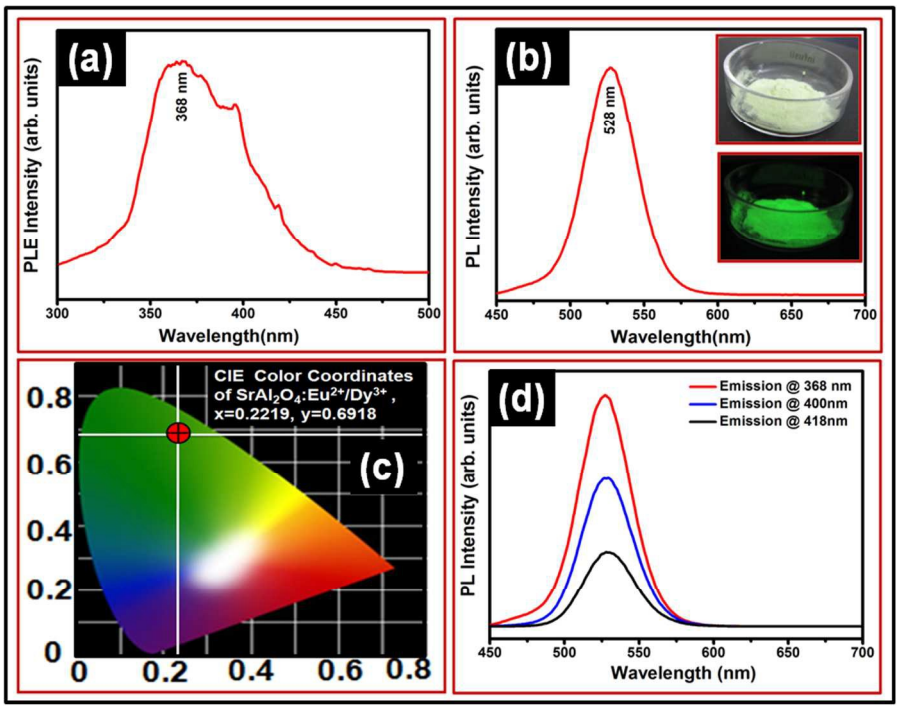

Fig. 4: (a) the excitation spectrum of $Sr_{0.7}Al_2O_4:Eu_{0.1}^{2+}/Dy_{0.2}^{3+}$ phosphor at 528 nm emission wavelength, presenting the maximum intensity peak at 368 nm, (b) the emission spectrum of $Sr_{0.7}Al_2O_4:Eu_{0.1}^{2+}/Dy_{0.2}^{3+}$ phosphor, peaking at 528 nm wavelength (greenish emission is ascribed to the $4f^65d^1 \rightarrow 4f^7$ electronic dipole allowed transition of Eu^{2+} ions located inside the $SrAl_2O_4$ host); inset shows the typical optical micrograph image of $Sr_{0.7}Al_2O_4:Eu_{0.1}^{2+}/Dy_{0.2}^{3+}$ phosphor (yellowish white color) under room light as well as an afterglow powder of $Sr_{0.7}Al_2O_4:Eu_{0.1}^{2+}/Dy_{0.2}^{3+}$ phosphor (a strong green color emission is appeared when 370 nm UV lamp is removed after 10 min), (c) the CIE color coordinates obtained from green emission spectra of $Sr_{0.7}Al_2O_4:Eu_{0.1}^{2+}/Dy_{0.2}^{3+}$ phosphor; x= 0.2219 and y=0.6918 and (d) PL spectra at different excitation wavelength (λ_{ex} = 368, 400 and 418 nm) of $Sr_{0.7}Al_2O_4:Eu_{0.1}^{2+}/Dy_{0.2}^{3+}$ phosphor, shows the strong green emission at 368 nm excitation wavelength.

emission radiation of a phosphor. The first is the strength of the host materials field at the sites of luminescent ions, and second is the degree of covalence of these ions with the surrounding oxygen ions. The role of the host material field is to split the 5d level into sublevels; the luminescence always takes place from the lowest sublevel.[29] The inset of Fig. 4b shows the typical optical micrograph image of $Sr_{0.7}Al_2O_4:Eu_{0.1}^{2+}/Dy_{0.2}^{3+}$ phosphor (yellowish white color) under room light as well as an afterglow powder of $Sr_{0.7}Al_2O_4:Eu_{0.1}^{2+}/Dy_{0.2}^{3+}$ phosphor (a strong green color emission is appeared, when 370 nm excitation source is removed after 10 mins). The relative intensity between the strontium aluminate host broad band and $4f^65d^1 \rightarrow 4f^7$ transition in Eu^{2+} strongly depend on the activation/deactivation of the host-to-electron-to-trapping centre energy-transfer processes, allowing the fine-tuning of the host emission chromaticity across the Commission Internationale d'Eclairage (CIE) diagram. The CIE color coordinates obtained from emission spectra of $Sr_{0.7}Al_2O_4:Eu_{0.1}^{2+}/Dy_{0.2}^{3+}$ phosphor are x= 0.2219 and y=0.6918, as shown in Fig. 4c, indicating the emission of the green color. This emission-color fine tuning along the CIE chromaticity diagram can be also modulated by chemical factors (Eu^{2+} / Dy^{3+} concentration, nature of the electrons and holes) and physical parameters (excitation wavelength and temperature). The optimization of PL of $Sr_{1-x-y}Al_2O_4:Eu_x^{2+}/Dy_y^{3+}$ phosphor has been achieved by several statistical runs for different concentration of Eu_x^{2+}/Dy_y^{3+} (x=0.05 to 0.3 and y=0.1 to 0.6), as presented in Fig. S1 (see supplementary information) and inset shows the maximum PL intensity with the different concentration of Eu^{2+} in $Sr_{1-x-y}Al_2O_4:Eu_x^{2+}/Dy_y^{3+}$ phosphor. The obtained results affirmed that the optimum sample was achieved for x=0.1 and y=0.2 mole percentage value in $Sr_{1-x-y}Al_2O_4:Eu_x^{2+}/Dy_y^{3+}$ formula. The emission intensity increases with respect to concentration of Eu, Dy, which is varying from x=0.05 to x=0.1& y=0.1 to 0.2 and arrive at the maximum intensity. Then, the emission intensity decreases once the concentration exceeds the optimum concentration (x=0.1 and y=0.2 mole percentage) of Eu and Dy, respectively. The incorporating appropriate amounts of Eu^{2+} and Dy^{3+} into $Sr_{1-x-y}Al_2O_4$ phosphor can significantly enhance the emission intensity due to the energy transfer and quenching phenomena at higher concentration of dopant ions Eu and co-dopant Dy. Fig. 4d exhibits the other emission spectra of $Sr_{0.7}Al_2O_4:Eu_{0.1}^{2+}/Dy_{0.2}^{3+}$ phosphor at 368, 400 and 418 nm excitation wavelengths, which are all effectively the same differing only in their intensity. It attributes an emission at 528 nm wavelength and maximum intensity is obtained for 368 nm excitation wavelength.

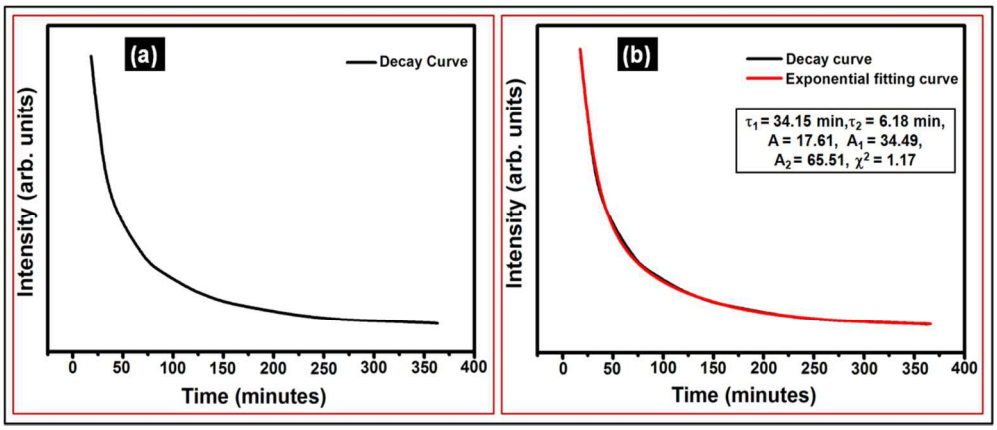

Fig. 5: (a) TRPL afterglow decay curve of $Sr_{0.7}Al_2O_4:Eu_{0.1}^{2+}/Dy_{0.2}^{3+}$ phosphor after 10 min excitation with a 368 nm wavelength xenon flash lamp, it reveals a very broad time framed emission for ~5 hours and (b) the exponential fitting of decay curve and inset shows the attenuation data parameter.

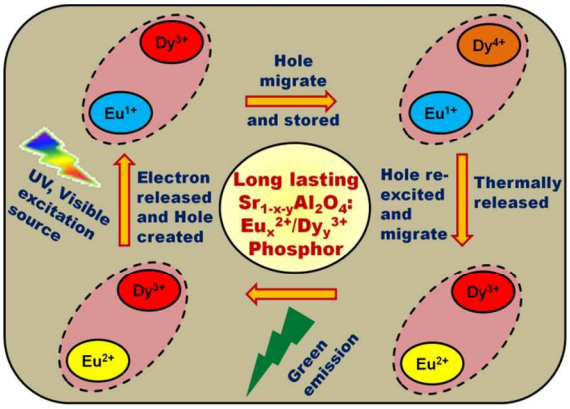

Fig. 6: The proposed mechanism of $Sr_{1-x-y}Al_2O_4:Eu_x^{2+}/Dy_y^{3+}$ green light emitting long persistent phosphor induced by the UV and visible excitation source.

Besides the intense PL, $Sr_{0.7}Al_2O_4:Eu_{0.1}^{2+}/Dy_{0.2}^{3+}$ phosphor also exhibits long lasting visible persistent luminescence after removal of the excitation source. The time-resolved photoluminescence (TRPL) decay profile of the phosphor was recorded with the help of time correlated single photon counting technique. The TRPL decay curve and exponentially fitting curves with attenuation data parameter of $Sr_{0.7}Al_2O_4:Eu_{0.1}^{2+}/Dy_{0.2}^{3+}$ phosphor monitored at 528 nm emission upon 368 nm excitation wavelength at room temperature is shown in Figs. 5a and b. The decay processes of phosphor possessed a double-exponential decay character. The decay behaviour of the phosphor can be fitted by an empirical equation stated as:

$$I = A_1 \exp(-t/\tau_1) + A_2 \exp(-t/\tau_2) \quad .....(1)$$

Where A_1& A_2 are the weighting constants parameters, t is the time period and τ_1& τ_2 are attenuation parameters for the exponential decay components. Using fitting functions, these parameters can be calculated by simulating the decay curves of the phosphors. The Fig. 5b demonstrates the exponential fitting of decay profile as described in equation (1). The parameters generated from fitting are listed in the inset of Fig. 5b. The exponential fitting generated parameters are τ_1 ~ 34.15 min and τ_2 ~ 6.18 min. It means, when the source lamp was switched off after 10 min, the intensity of the afterglow firstly decreases rapidly within 1 hour and subsequently forms a stable long persistent emission more than 5 hours. The effect of dopant concentration on the afterglow properties was evaluated by varying the concentration of Eu^{2+} and Dy^{3+} in $Sr_{1-x-y}Al_2O_4:Eu_x^{2+}/Dy_y^{3+}$ (x= 0.05 to x=0.3, y=0.1 to 0.6) phosphor.

The decay curves of all variants of $Sr_{1-x-y}Al_2O_4:Eu_x^{2+}/Dy_y^{3+}$ (x= 0.05 to x=0.3, y=0.1 to 0.6) phosphors are depicted in Fig. S5 (see supplementary information) after 10 min excitation with a 368 nm wavelength xenon flash lamp. These results are good consistent with the PL emission data. The observed enhancement of afterglow intensity can be attributed to the presence of sufficient number of shallow traps in Eu^{2+} ions while lengthening of decay times is ascribed to the deeper trap density of Dy^{3+} ions into the host lattice. This trap–transport–detrap process results in the long-afterglow phenomenon of the synthesized phosphor and the proposed model is illustrated in Fig. 6. It significantly improves the long lasting luminescence of such phosphors that is more favorable in upcoming potential applications, as given below.

3.4. Exploration of $Sr_{1-x-y}Al_2O_4:Eu_x^{2+}/Dy_y^{3+}$ phosphor in optical display applications

The $Sr_{1-x-y}Al_2O_4:Eu_x^{2+}/Dy_y^{3+}$ phosphor was generated on the ceramic based Tajmahal under room conditions for optical display applications. The as obtained thick transparent solution (as explained in experimental section) was used as a luminous paint at room temperature in the laboratory. The luminous paint was coated onto the ceramic based Tajmahal using spray machine and was left in the open air to dry in the laboratory at room temperature. The obtained proto-type Tajmahal was excited by white fluorescent tube light for 5 min. and it exhibits afterglow for several hours after the source was ceased off. This

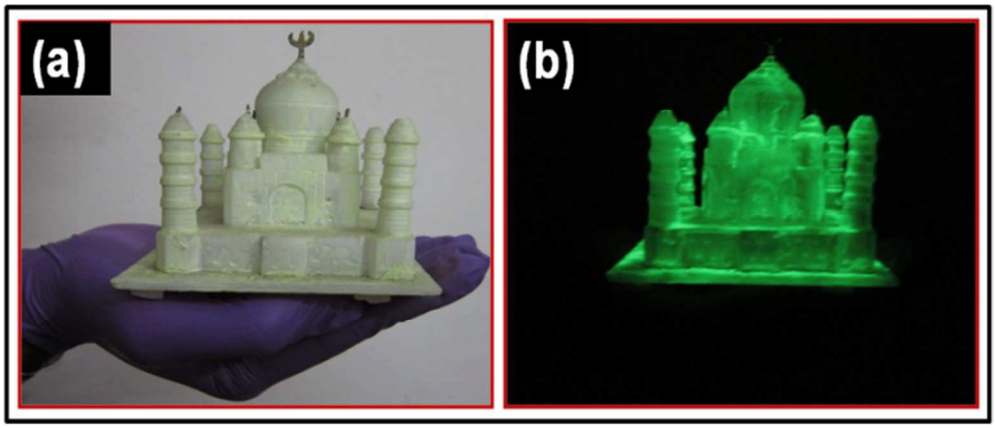

Fig. 7: The optical image of $Sr_{0.7}Al_2O_4:Eu_{0.1}^{2+}/Dy_{0.2}^{3+}$ phosphor coated Tajmahal monument in room light and (b) optical image of afterglow Tajmahal monument in dark medium, when the white fluorescent tube light was switched off after 5 min.

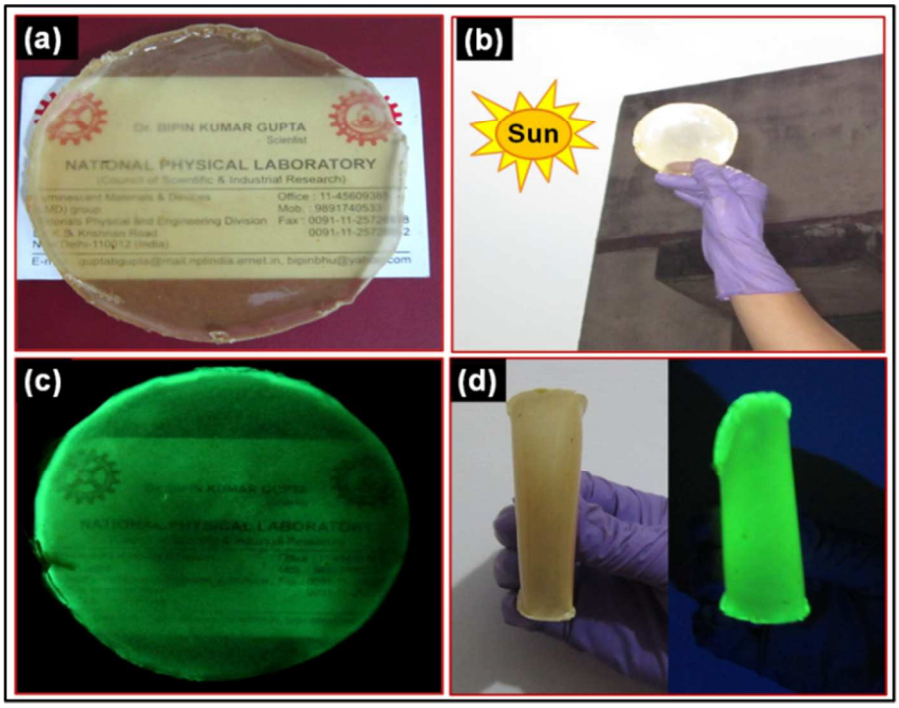

Fig. 8: (a) The optical photograph of $Sr_{0.7}Al_2O_4:Eu_{0.1}^{2+}/Dy_{0.2}^{3+}$ phosphorescent layer with better transparency ~76%, (b) sunlight activation of $Sr_{0.7}Al_2O_4:Eu_{0.1}^{2+}/Dy_{0.2}^{3+}$ phosphor layer which is rapidly charged within 5 min, (c) $Sr_{0.7}Al_2O_4:Eu_{0.1}^{2+}/Dy_{0.2}^{3+}$ phosphorescent layer emits a strong green afterglow emission in dark medium and (d) left optical image indicates the high flexibility of layer and right optical image also shows the afterglow green emission layer with same flexibility.

proto-type Tajmahal works for display purpose, as shown in Fig. 7, where Fig. 7a represents optical image of $Sr_{0.7}Al_2O_4:Eu_{0.1}^{2+}/Dy_{0.2}^{3+}$ phosphor coated Tajmahal monument in room light and Fig. 7b exhibits optical image of afterglow Tajmahal monument in dark medium, when the excitation source white fluorescent tube light was switched off after 5 min.

3.5. Exploration of $Sr_{1-x-y}Al_2O_4:Eu_x^{2+}/Dy_y^{3+}$ phosphor in defence applications

The as-prepared phosphorescent layer (as explained in experimental section) was further used in defence applications. The optical photograph of $Sr_{0.7}Al_2O_4:Eu_{0.1}^{2+}/Dy_{0.2}^{3+}$ phosphorescent layer is given in Fig. 8a with better transparency ~76%. Figs. 8b and 8c show that the $Sr_{0.7}Al_2O_4:Eu_{0.1}^{2+}/Dy_{0.2}^{3+}$ phosphorescent layer can be effectively activated and rapidly charged by direct sunlight for 5 min and emits a strong green afterglow emission in dark medium, respectively. Fig. 8d depicts the left optical image having high flexibility of layer after several statistical folding. It can be fold upto 360^0 without any kind of deformation in the layer. The right optical image (Fig.

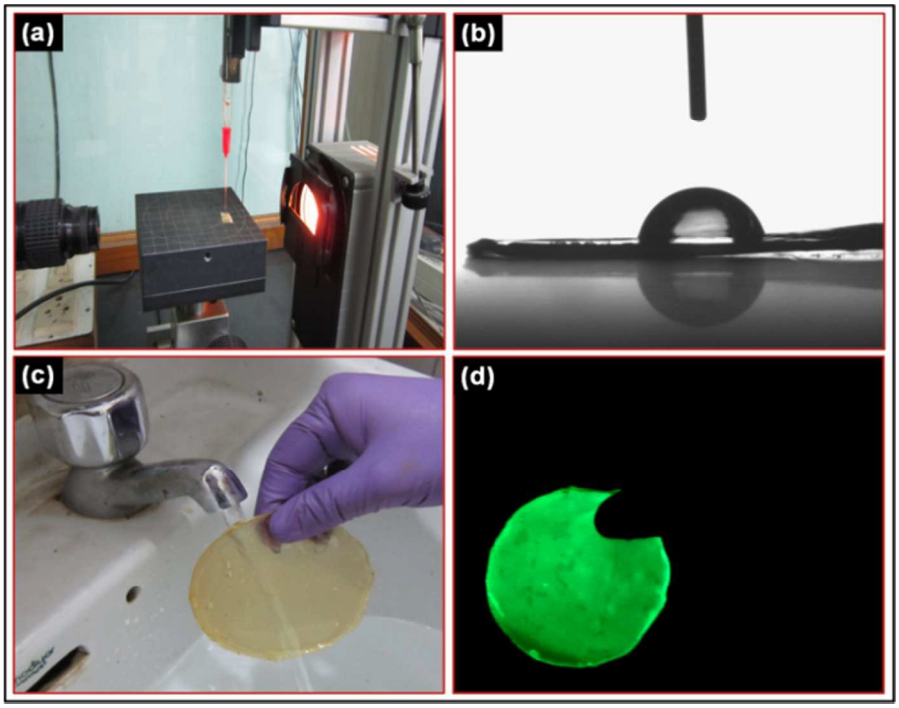

Fig. 9: (a) contact angle measurement setup, (b) optical image showing water droplets for contact angle measurement, after drop interact with upper surface of $Sr_{0.7}Al_2O_4:Eu_{0.1}^{2+}/Dy_{0.2}^{3+}$ phosphorescent layer and spread out, measured contact angle is 70°, (c) optical image of $Sr_{0.7}Al_2O_4:Eu_{0.1}^{2+}/Dy_{0.2}^{3+}$ phosphorescent layer washed under tap water for 5 min and (d) afterglow green emission of layer with same intensity when exposed under sunlight for 5 min.

8d) also shows the afterglow green emission layer with same flexibility. The activation process doesn't affect the flexibility of layer.

The hydrophobic nature of phosphorescent layer was also examined using contact angle measurement. It can be found using the measurement setup, as shown in Fig. 9a. The whole measurement setup is depicted in Fig. S6 (see supplementary information). The contact angle between layer and water droplet is about 70° (Fig. 9b) and water is easily spread out on phosphorescent layer. It is absorbed through the within few second. When layer is washed under tap water (Fig. 9c) for 5 min and fully charged within 5 mins of exposure to sunlight, emits again afterglow green emission with same intensity (Fig. 9d). It means, the degradation of material from the layer washing process doesn't occur. Thus, this flexible, transparent and water **resistant** afterglow phosphorescent layer can be used in defence applications.

A optical image of long size (11inch X 12inch) of $Sr_{0.7}Al_2O_4:Eu_{0.1}^{2+}/Dy_{0.2}^{3+}$ long lasting phosphorescent layer is also prepared easily under the room temperature conditions to design the soldier jacket (Fig. 10a), which can be used in coal mining and military persons. This long layer shows the same afterglow green emission of $Sr_{0.7}Al_2O_4:Eu_{0.1}^{2+}/Dy_{0.2}^{3+}$ long lasting phosphorescent layer with high intensity (Fig. 10b), after exposed under sunlight for 5 min. The optical images of dummy soldier without and with phosphorescent jacket are given in Figs. 10c and 10d, respectively. The phosphorescent jacket covered with dummy soldier was then kept in the sunlight for 5 min and visualize the phosphorescent jacket in dark medium with strong green emission (Fig. 10e). Thus, these above mentioned purposed applications (better transparency, high flexibility, water **resistant** and decorative) reflect the novelty of this $Sr_{1-x-y}Al_2O_4:Eu_x^{2+}/Dy_y^{3+}$ phosphor. Moreover, it can be also used in some other potential application such as emergency signs, buildings and highways, plasma display panels, LEDs, textile and luminous paints etc.

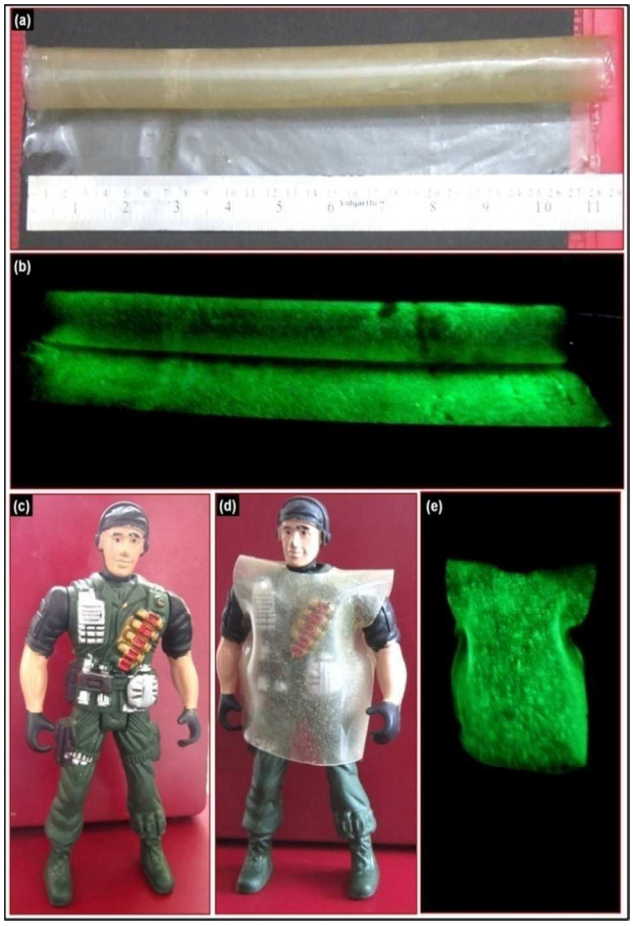

Fig. 10: (a) The optical image of long size (11inch X 12inch) of $Sr_{0.7}Al_2O_4:Eu_{0.1}^{2+}/Dy_{0.2}^{3+}$ long lasting phosphorescent layer (b) afterglow green emission of $Sr_{0.7}Al_2O_4:Eu_{0.1}^{2+}/Dy_{0.2}^{3+}$ long lasting phosphorescent layer with high intensity after exposed under sunlight for 5 min, (c) optical image of dummy soldier without, (d) with phosphorescent jacket and (e) the phosphorescent jacket covered with dummy soldier in dark medium with strong green emission.

4. Conclusions

In summary, we have successfully demonstrated a series of $Sr_{1-x-y}Al_2O_4:Eu_x^{2+}/Dy_y^{3+}$ long persistent phosphors that can be effectively activated by UV, white fluorescent tube light and sun radiation, exhibiting an extremely long lasting afterglow more than 5 hours emission. The XRD analysis confirmed the formation of homogeneous single phase of monoclinic $SrAl_2O_4$ crystal structure. The PL spectrum exhibits a hyper-intense green emission peaking at 528 nm corresponding to $4f_65d_1$-$4f_7$ transition of Eu^{2+} and color co-ordinates are x= 0.2219 and y=0.6918. The long afterglow characteristics of $Sr_{1-x-y}Al_2O_4:Eu_x^{2+}/Dy_y^{3+}$ persistent phosphors can be attributed to the electron and hole trapped-transported de-trapped process. Thus, the obtained $Sr_{1-x-y}Al_2O_4:Eu_x^{2+}/Dy_y^{3+}$ phosphor with relatively high initial brightness, long lasting time, high intense emitting green color, transparency, water **resistant** and flexibility properties in phosphorescent layer ensure their potential applications as in display and defence.

Notes and references

[a] *CSIR - National Physical Laboratory, Dr K S Krishnan Road, New Delhi, 110012, India*
[b] *Department of Physics, University of Rajasthan, Jaipur, 302055, India*

* *Corresponding author. Tel.: +91-11-45609385, Fx: +91-11-45609310*
E-mail address: ***bipinbhu@yahoo.com***

Acknowledgments

The authors wish to thank Prof. R. C. Budhani, Director, N.P.L., New Delhi for his keen interest in the work. The authors gratefully acknowledged University Grant Commission (UGC) and Council of Scientific and Industrial Research (CSIR), Govt. of India for financial assistance to carry out this work.

References:

1 G. Fang, X. Zhaoxian, X. Hao and L. Yongxi, *J. Phys.: Conf. Ser.*, 2009, **152**, 012082.
2 A. Bessière, S. K. Sharma, N. Basavaraju, K. R. Priolkar, L. Binet, B. Viana, A. J. J. Bos, T. Maldiney, C. Richard, D. Scherman and D. Gourier, *Chem. Mater.*, 2014, **26**, 1365−1373.
3 R. Chen, Y. Hu, L. Chen, X. Wang, Y. Jin and H. Wu, *Ceram. Int.*, 2014, **40**, 8229–8236.
4 J. Ueda, K. Aishima, S. Nishiura and S. Tanabe, *Appl. Phys. Express*, 2011, **4**, 042602.
5 W. Wang, P. Yang, Z. Cheng, Z. Hou, C. Li and J. Lin, *ACS Appl. Mater. Interfaces*, 2011, **3**, 3921–3928.
6 Y. Tang, H. Song, Y.Su and Y. Lv, *Anal. Chem.*, 2013, **85**, 11876−11884
7 M. Kowatari, D. Koyama, Y. Satoh, K. Iinuma and S. Uchida, *Nucl. Instrum. Methods Phys. Res., Sect. A*, 2002, **480**, 431−439.
8 Z. Hosseini, W. K. Huang, C. M. Tsai, T. M. Chen, N. Taghavinia and E. W. G. Diau, *ACS Appl. Mater. Interfaces*, 2013, **5**, 5397−5402
9 W. He, T.S. Atabaev, H. K. Kim and Y. H. Hwang, *J. Phys. Chem. C*, 2013, **117**, 17894−17900.
10 X. Huang, S. Han, W. Huang and X. Liu, *Chem. Soc. Rev.*, 2013, **42**, 173−201.
11 T. Aitasalo, P. Deren, J. H. lsa, H. Jungner, J. C. Krupa, M. Lastusaari, J. Legendziewicz, J. Niittykoski and W. Strek, *J. Solid State Chem.*, 2003, **171**, 114–122.
12 Y. H. Lin, Z. L. Tang, Z. T. Zhang, X. X. Wang and J. Y. Zhang, *J. Mater. Sci. Lett.*, 2001, **20**, 1505−1506.
13 T. Matsuzawa, Y. Aoki, N. Takeuchi and Y. Murayama, *J. Electrochem. Soc.*, 1996, **143**, 2670-2673.
14 X. J. Wang, D. D. Jia and W. M. Yen, *J. Lumin.*, 2003, **102**, 34−37.
15 X. Xu, Y.Wang, Y. Li and Y. Gong, *J. Appl. Phys.*, 2009, **105**, 083502.
16 P. F. Smet, I. Moreels, Z. Hens and D. Poelman, *Mater.*, 2010, **3**, 2834−2883.
17 M. Peng and G. Hong, *J. Lumin.*, 2007, **127**, 735−740.
18 C. Zhao, D. Chen, Y. Yuan and M. Wu, *Mater. Sci. Eng. B*, 2006, **133**, 200–204.
19 V. P. Singh, S. B. Rai, H. Mishrac and Chandana Rath, *Dalton Trans.*, 2014, **43**, 5309–5316.
20 K. S. Hwang, B. A. Kang, S. D. Kim, S. Hwangbo and J. T. Kim, *Bull. Mater. Sci.*, 2011, **34**, 1059–1062.

21 M. P. Anesh, S. K. H. Gulrez, A. Anis, H. Shaikh, M. E. Ali Mohsin and S. M. AL-Zahrani, *Adv. Polym. Technol.*, 2014, DOI: 10.1002/adv.21436.

22 Y. Zhang, Z. Chen and Z. Zhou, *J. Electrochem. Soc.*, 2006, **153**, H86–H87.

23 Y. F. Xu, D. K. Ma, M. L. Guan, X. A. Chen, Q. Q. Pan and S. M. Huang, *J. Alloys Compd.*, 2010, **502**, 38–42.

24 Y. H. Lin, Z. L. Tang and Z. T. Zhang, *Mater. Lett.*, 2001, **51**, 14–18.

25 O. M. Ntwaeaborwa, P. D. Nsimama, S. Pitale, I. M. Nagpure, V. Kumar, E. Coetsee, J. J. Terblans and H. C. Swart, *J. Vac. Sci. Technol. A*, 2010, **28**, 901-905.

26 G. Kedawat, S. Srivastava, V. K. Jain, Pawan, V. Kataria, Y. Agrawal, B. K. Gupta and Y. K. Vijay, *ACS Appl. Mater. Interfaces*, 2013, **5**, 4872-4877.

27 B. K. Gupta, D. Haranath , S. Saini, V. N. Singh, V. Shanker, *Nanotechnol.*, 2010, **21**, 055607.

28 F. Clabau, X. Rocquefelte, S. Jobic, P. Deniard, M. H. Whangbo, A. Garcia and T. L. Mercier, *Solid State Sci.*, 2007, **9**, 608–612.

29 D. Haranath, V. Shanker, H. Chander and P. Sharma, *J. Phys. D: Appl. Phys.*, 2003, **36**, 2244–2248.

30 N. Tyagi, D. S. Jo, T. Abe, K. Toda, S. J. Lee, S. G. Oh, T. Masaki and D. H. Yoon, *J. Lumin.*, 2014, **147**, 245–249.

Table S1: The studied sample compositions of the $Sr_{1-x-y}Al_2O_4:Eu_x^{2+}/Dy_y^{3+}$; x= 0.05 to x=0.3, y=0.1 to y=0.6 phosphor powder

x	y	$Sr_{1-x-y}Al_2O_4:Eu_x^{2+}/Dy_y^{3+}$
0.05	0.1	$Sr_{0.85}Al_2O_4:Eu_{0.05}^{2+}/Dy_{0.1}^{3+}$
0.1	0.2	$Sr_{0.7}Al_2O_4:Eu_{0.1}^{2+}/Dy_{0.2}^{3+}$
0.15	0.3	$Sr_{0.55}Al_2O_4:Eu_{0.15}^{2+}/Dy_{0.3}^{3+}$
0.20	0.4	$Sr_{0.4}Al_2O_4:Eu_{0.20}^{2+}/Dy_{0.4}^{3+}$
0.25	0.5	$Sr_{0.25}Al_2O_4:Eu_{0.25}^{2+}/Dy_{0.5}^{3+}$
0.3	0.6	$Sr_{0.1}Al_2O_4:Eu_{0.3}^{2+}/Dy_{0.6}^{3+}$